An Enhanced Acute Leukemia Segmentation based on Particle Swarm Optimization

Nor Hazlyna.H, Muhammad Khusairi.O, Muhamad Fitri Zakwan.Y, Hamirul Aini.H, M.Y.Mashor, R. Hassan, R.A.A.Raof

Abstract: One of the hemopoietic disorders in humans is acute leukemia. Cell growth in acute leukemia disease occurs rapidly and uncontrollably. Therefore, in order to maximize the efficacy of treatment, there is a need to detect the disease early. Recently, Computer-Aided Detection and Diagnosis (CAD) approaches have been developed to assist medical staff in interpreting medical images. A crucial CAD technique for the diagnosis and verification of diseases such as acute leukemia is image-segmentation. However, it is still challenging to segment acute leukemia cells from the background due to the inconsistency of intensity image for acute leukemia blood samples. The original acute leukemia image firstly utilizes the formula of saturation with reference to the colour spaces of the HSI. Subsequently, the S-component is obtained and fed into the PSO to perform the segmentation process. Besides that, in order to optimize the segmentation process and increase the detection accuracy, the k-means algorithm is proposed as the initial centroid for PSO, called hybrid k-means-PSO. The proposed methods are performed on 10 and 24 images of Acute Lymphocytic Leukemia (ALL) as well as Acute Myelogeneous Leukemia (AML) respectively, which have been captured using an Infinity2 camera mounted on Leica microscope. The k-means clustering are used as the reference standard for the performance evaluation. Simulation results indicate that both PSO and hybrid k-means-PSO methods have better accuracy compared to k-means with the highest accuracy obtained scoring up to 97.24% and 97.02% respectively. As a result, the proposed method can automatically segment acute leukemia cells from the background and is helpful for the classification stage.

Keywords: Acute Leukemia Blood Cell ImagesPSOMedical Image SegmentationS-Component ImageHybrid K-means -PSO Image Segmentation

Revised Manuscript Received on May 22, 2019.

Nor Hazlyna.H, Data Science Research Lab, School of Computing, College of Arts and Science, Universiti Utara Malaysia, 06100 Sintok, Kedah, Malaysia

Muhammad Khusairi.O, Faculty of Electrical Engineering, Universiti Teknologi MARA (UiTM), Jalan PermatangPauh, 13500 PermatangPauh, Pulau Pinang, Malaysia

Muhamad FitriZakwan.Y, Faculty of Electrical Engineering, Universiti Teknologi MARA (UiTM), Jalan PermatangPauh, 13500 PermatangPauh, Pulau Pinang, Malaysia

HamirulAini.H, Data Science Research Lab, School of Computing, College of Arts and Science, Universiti Utara Malaysia, 06100 Sintok, Kedah, Malaysia

M.Y.Mashor, School of Mechatronics Engineering, Universiti Malaysia Perlis, Pauh, Perlis, Malaysia.

R. Hassan, Department of Hematology, Universiti Sains Malaysia, Kubang Kerian, Kelantan, Malaysia

R.A.A.Raof, School of Computer & Communication Engineering, Universitit Malaysia Perlis

I. INTRODUCTION

Leukemia is known as a malignant progressive disease; also known as a cancer of the blood. The cause of leukemia is due to other blood forming organs and the bone marrow producing more than the usual number of leukocytes or White Blood Cell (WBC) which disables its infection-neutralizing ability. Generally, leukemia is of two types, namely acute and chronic. The term 'acute' refers to the progress and development of the disease that occurs rapidly [1, 2].

Acute leukemia can be divided into Acute Myelogeneous Leukemia (AML) as well as acute lymphocytic leukemia (ALL) [3], the latter of which is the commonest leukemia type in children. As for adults, those aged 65 and above have the highest risk of suffering from this condition.

On the other hand, the occurrence of AML is more in adults than children, especially men [4]. Chronic leukemia also consists of two types, namely Chronic Lymphocytic Leukemia (CLL) and Chronic Myelogeneous Leukemia (CML). If early detection has been made, it is possible to cure this disease if early treatment is applied.

In order to detect leukemia, the defective WBC count in the blood sample needs to be analyzed by the hematologist. Generally, in leukemia diagnosis, there are specific features that are considered such as shape and size of abnormal WBC that would be observed by the hematologist to determine the leukemia type [5, 6]. Complete Blood Count (CBC) is the initial step in the detection of leukemia. Abnormalities in the count can determine whether or not the patients will need to have their bone marrows biopsied. In terms of the hematologists' manual diagnoses, due to the human condition where people tend to make mistakes from natural habits such as tiredness and operator capabilities, the result obtained can be degraded [7].

As a way to improve the reliability of the result and help the hematologists in their field of work, a computer-based image processing method was introduced with the purpose of classifying and investigating acute leukemias. The extent to which an image is accurately segmented is the key of success for the proposed method. From the past few years, image segmentation plays an important role for fast detection of leukemia. Numerous image-segmentation techniques have been proffered as well as developed in the past. Methods such as c-means clustering [8], watershed transform [9], fuzzy based [10] and histogram thresholding [11] are some of the examples of the image segmentation method applied for leukemia detection.

One of the most popular image segmentation methods that has been proposed is *k*-means clustering [12] which produced a good accuracy. *k*-means clustering is a technique which employs the intensities to classify an image's pixels [13, 14].

Subrajeet et al. [8] utilized the c-means clustering algorithm extended method of *k*-means to segment lymphocyte images. This. The method was applied on 165 samples of blood smear images and achieves 95% accuracy. In another study, a watershed transform method was proposed by Bhattacharjee et al. [9] in 2015 to diagnose the ALL presence in blood smears accurately. A total of 45 samples of the blood slides images was used and able to obtain 95.56%. Accuracy for an automated leukemia, the fuzzy based detection proposed by Mohapatra et al. [10] used 108 images of blood smears, with an accuracy 93% of accuracy. Using 108 samples of the blood slide images, Joshi et al. [11] employed the Otsu's threshold technique of blood cell segmentation to detect the ALL in the blood. This method gives 93% of accuracy of the image segmented. The commonly used conventional method is *k*-means clustering. In 2013, Mohammed et al. [12] proposed this segmentation method. A sample of 440 lymphocyte images was used, where 12 were employed for Support Vector Machine (SVM) training while 140 to measure the precision of segmentation. The highest accuracies were 98.43% and 98.69% for nuclear and cellular segmentations respectively.

PSO is a new segmentation method that is inspired by the behavior of flocks of birds. Certain random molecules initialize the PSO, after which the latter identifies a global optimum by making updates in the position and velocity of particles. All particles are made to fly past the place of searching. The particles' positions are then modified with reference to the distances from their respective ideal positions as well as (2) the best-performing particle among them [15]. PSO is one of the popular methods used for tuning and optimizing a data. The results obtained from using this method show quite a high number in accuracy. PSO has been applied in many applications as an optimization tool such as in biological or medical science [16], signal processing, data mining, robotics and neural networks [17].

In medical imaging, PSO is utilized to segment images. Abdenour et al. proposed an improved c-means clustering by using the PSO algorithm for the segmentation of Magnetic Resonance (MR) images. The outcomes confirm the effectiveness of the proposed algorithm. A multilevel thresholding method as per the Fractional-Order Darwinian Particle Swarm Optimization (FODPSO) was introduced to segment the hyperspectral and multispectral images by Pedram et al. [19] in 2014. In 2012, Moradi et al. [20] presented a new combination of Genetic Algorithms (GA) / Particle Swarm Optimizations (PSO) to optimally locate and size the DG in the distributive systems. Some 33 as well as 69 bus systems were subjected to performance analyses to determine the efficacy of the combinatory algorithm. This proposed method shows a good result in this field.

Even though PSO has been widely applied in many applications of medical imaging, there are a few researches conducted for both types (AML and ALL images) of acute leukemia image segmentation. Two Bare-bones Particle Swarm Optimization (BBPSO) was used by WorawutSrisukkham et al., [21] to perform only for ALL type for the segmentation stage. The proposed algorithm was subsequently employed to ascertain the most salient feature that could differentiate deformed from normal ALL cells. Evidently, the achieved geometric average efficacies were 94.94% as well as 96.25% respectively.

Besides that, the Co-operative Multiswarm Particle Swam Optimization (CMPSO) was employed by PrativaAgarwalla and Sumitra Mukhopa [22] using the DNA Array to identify the clusters of cancer-associated genes that were coregulated. The said method was used on a dataset that was an important contributor to the detection of pediatric leukemias.

Therefore, this study proposes to deal with the strength of PSO for both types of acute leukemia (AML and ALL types) for robust segmentation. On top of that, the study also proposes combining the PSO with *k*-means, called hybrid *k*-means-PSO, to improve the segmentation process. Then, to ease the acuteleukemia segmentation process, the saturation component of the HSI colour model is proposed in this study. Finally, these proposed methods were compared with the conventional *k*-means method and their performances were evaluated. This method is a platform for further research to assist hematologists in diagnosing acute leukemia disease based on blood samples.

II. METHODOLOGY

Our proffered method comprised three main steps: (a) RGB to HSI colour model conversion, (b) extraction of S-component based on HSI colour model, and (c) acute leukemia image segmentation. Fig. 1 shows the illustration of the flowchart for the image processing technique applied. In the acute leukemia image segmentation stage, two types of image segmentation were applied, PSO and hybrid *k*-means-PSO. The detailed description of the proposed image segmentation steps will be discussed in the following sections.

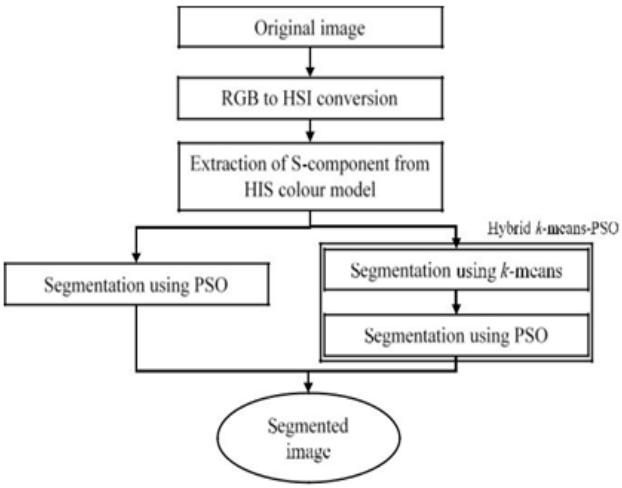

Fig. 1 The proposed leukemia image segmentation procedure using PSO

Published By:
Blue Eyes Intelligence Engineering
& Sciences Publication

Image Acquisition

The acute leukemia blood samples used for this project came from the Hematological Department of Hospital Universiti Sains Malaysia (HUSM), Kelantan. The blood slide of acute leukemia was analysed using the Leica microscope with 40X magnifications. Then, 10 ALL and 24 AML images were captured respectively from the blood samples, after which they were saved in the form of (.*bitmap) at a resolution of 800 × 600 using the Infinity2 camera.

Saturation Based on HSI Colour Space

The threshold selection method utilized the saturation formula with reference to the colour model of HIS which comprised saturation, intensity as well as hue. The last component in HSI represents the impression which is associated with the wavelength that predominates in the colour stimulus. Meanwhile, saturation refers to the extent of addition of white light to a pure colour. Intensity refers to an image's brightness. The S-component-based segmentation was chosen as it shows the best result for image segmentation where a clear view of the acute leukemic cell as well as a prominent S-component image was possible [23]. In the S-component image, the saturation of the RBCs as well as the undesired background enabled more accurate segmentations. The RGB-to-HSI colour model conversion was performed with respect to the equations below:

$$Hue = \frac{\cos^{-1}\left(0.5\times\left((R-G)+(R-B)\right)\right)}{\left((R-G)^2+(R-B)\times(G-B)\right)^{0.5}} \quad (1)$$

$$Sat = 1 - \frac{3}{(R+G+B)} min(R+G+B) \quad (2)$$

$$Int = \frac{1}{3(R+G+B)} \quad (3)$$

Where R, G, and B denote the intensities of red, green, and blue in the RGB colour model. Fig. 2 shows examples of conversion. It can be observed that the WBCs are more obvious in terms of their saturation component image, where 2(c) is better compared to the hue of 2(b) and intensity in the 2(d) component. This indicates that the S-component provides the most important information for segmenting the acute leukemia cells compared to the H- as well as I-components.

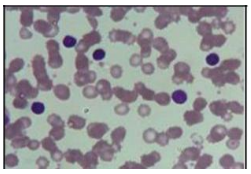

(a) Original image

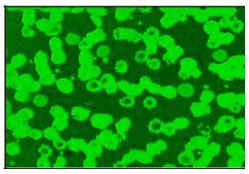

(b) H-component mage

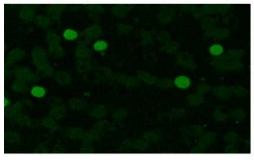

(c) S-component image

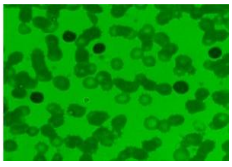

(d) I-component image

Fig. 2 (a) Original Image (b) H-component image (c) S-Component image (d) I-component image

Particle Swarm Optimization

After obtaining the S-component based on the HSI colour model, the image was taken over by the PSO to finish the segmentation process. Using PSO, the undesired portions of the image (i.e. RBCs and background noise) and only the abnormal WBC were left for the analysis. The segmented image was compared with the ground truth images. The data was tabulated in a table for the record. The recorded data was compared with the previous invented method of *k*-means in terms of the accuracy and time taken for the process done. The method for PSO segmentation is described below:

1. All particles are initialized to N_c randomly-selected cluster centroids.
2. From $t = 1$ to the number of iterations
   a) For every particle, i
   b) For every data vector, z_p
   i. The Euclidean distance, $d(z_p, m_{ij})$, to all cluster centroids, Cij, is calculated as per Equation 4.

$$d(z_p, m_j) = \sqrt{\sum_{k=1}^{N_d} (z_{pk} - m_{jk})^2} \quad (4)$$

here d denotes the distance to the centroids, Z_p the p^{th} data vector, m_j the centroid vector of cluster j, as well as N_d the dimensions of input.

ii. To cluster C_{ij}, z_p is assigned to give $d(Z_p, m_{ij}) = min_{vc=1,\dots,No}$[17]

Fitness is calculated with reference to Equation 5.

$$J_6 = \frac{\sum_{j=1}^{Nc}[\sum \forall Z_p \in C_{ij} d(z_p, m_j)/|C_{ij}|]}{N_C} \quad (5)$$

where N_c refers to the centroid count and $|C_{ij}|$ the quantity of data vectors that belong to C_{ij}. The definition of d has been provided in Equation 4.

a) The ideal global and local positions are updated as per Equation 6.

$$Y_{id} = \begin{cases} Y_{id}, & if\ f(X_i) \geq f(Y_i) \\ X_{id}, & if\ f(X_i) < f(Y_i) \end{cases} \quad (6)$$

where Y_i denotes a specific particle's ideal position and X_i the particle's present location.

b) The cluster centroids are updated as per Equations 7 and 8.

$$V_{id} = WV_{id} + C_1R_1(P_{id} - X_{id}) + C_2R_2(P_{gd} - X_{gd}) \quad (7)$$

$$X_{id} = X_{id} + V_{id} \quad (8)$$

With reference to Equation 7 and Equation 8, V_i and X_i denote the velocity and position of particles I respectively, W the inertial weight, C_1 and C_2 the cognition and social factors respectively, R_1 and R_2 the uniformly-distributed random numbers ranging from 0 to 1, Pi and Pg the pbest and gbest respectively.

Published By:
Blue Eyes Intelligence Engineering
& Sciences Publication

Steps (a) to (d) were repeated to attain an iteration of 100. In this study, 0.72, 1.49 and 1.49 were assigned to W, C_1, and C_2 respectively since they were appropriate for use in numerous applications as suggested in [17]

Hybrid k-means-PSO

Ensuring the effectiveness of the segmentation method by using hybrid *k*-means-PSO – which was an amalgamation of the existing *k*-means technique and PSO – was put forward as well. After obtaining the *S*-component image, the segmentation using the *k*-means was applied. *k*-means clustering is an unsupervised method. For this hybrid *k*-means-PSO method, the use of *k*-means is to provide a primary segmentation of the image. *k*-means clustering is used because it is simple and has relatively low computational complexity. In addition, it is suitable for biomedical image segmentation. The value of *k* selected is 2, which represents the WBC and other background components including the RBC. Initial cluster centers are chosen in a first pass of the data. The dataset is partitioned into *k* clusters and the data points are randomly assigned to the clusters resulting in clusters that have roughly the same number of data points. For each data point, the Euclidean distance from the data point to the mean of each cluster will be calculated. If the data point is not closest to its own cluster, it will have to be shifted into the closest cluster. If the data point is already closest to its own cluster, then it will not be shifted. The process continues until cluster means do not shift more than a given cut-off value or the iteration limit is reached. Based on the segmentation of *k*-means, PSO will use the centroid value of *k*-means and optimize the value in order to improve the segmentation processed. The method is also able to avoid the inaccurate clustering of *k*-means [24]. The pseudo-code of the proposed hybrid *k*-means-PSO is shown as below:

1. Let $C=\{c_j \mid j=1,2,\ldots., K\}$ represents a set of K intensities for initial centres.
2. Calculate the intensity difference between each pixel and the pixel centres as per Equation 9.

$$d_{ij} = \left\| x_i - c_j \right\| \tag{9}$$

3. Assign the pixel to its closest centre.
4. When all pixels have been assigned, recalculate the new positions of the centres, *cj* according to:

$$c_j = \frac{\sum_{i=1}^{N_{c_j}} x_{i,c_j}}{N_{c_j}} \tag{10}$$

Where x_{i,c_j} and N_{c_j} represent the intensity of the *i*-th pixel and the number of pixels belong to centre, c_j respectively.

5. Repeat Step 1-5 until the position of all centres does not move at all.
6. Assign each particle to N_c using cluster centroid obtained by *k*-mean clustering operation.
7. Perform Step 1-2 in Section 1.3. The process is repeated until stopping criteria is met.

III. RESULTS AND DISCUSSION

For the proposed method, 34 images were obtained from 9 ALL and AML slides chosen for the image segmentation test using the PSO method. Fig. 3(a) and 4(a) show the images that were originally captured from the slide of ALL blood samples. The resolution for the captured image is 800x600 with the bitmap format (.bmp).

The purpose of the conversion is to enable the extraction of the saturation component (S) value to obtain the *S*-component image as illustrated in Fig. 3(c) and 4(c). The final step for the image segmentation was done by the PSO. Fig. 3(d) and 4(d) display the product of segmentation by PSO. When checking the segmented image's accuracy, the ground truth images as in Fig. 3(e) and 4(e) were used as a reference to calculate the percentage of similarity. The accuracy test was done using a MATLAB program called the structural similarity index (SSIM). The percentages of similarity between the segmented image for Fig.3 are 97.93% and 97.88%. In the same test, the similarity percentages for the image segmented by using *k*-means are 97.59% for Fig. 3 and 96.91% for Fig. 4. For images segmented by the hybrid method, the results of the similarity percentage for Fig. 3 were 98.50% and 98.29% for Fig. 4.

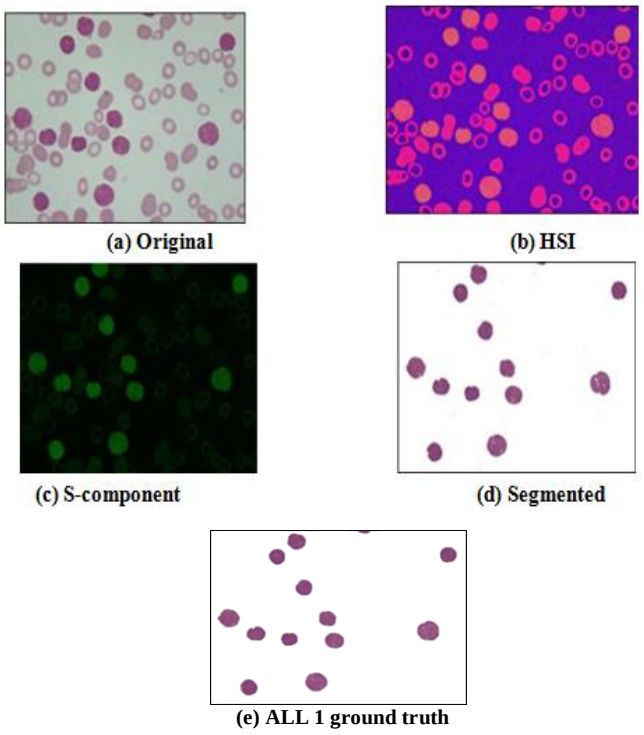

Fig. 3 ALL 1 imagess: (a) Original (b) HIS (c) S-component (d) Segmented (e) ALL 1 ground truth

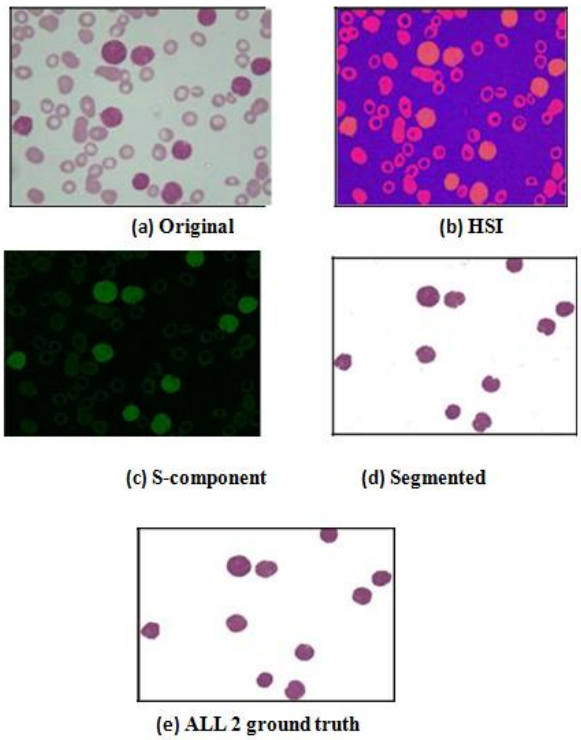

Fig. 4 ALL 2 images: (a) Original (b) HIS (c) S-component (d) Segmented (e) ALL 2 gsround truth

Fig. 5(a) and 6(a) show the original AML images. The HSI that has been converted for this sample is as displayed in Fig. 5(b) and 6(b). *S*-component was extracted and the images are as shown in Fig. 5(c) and 6(c). Then, Fig. 5(d) and 6(d) show the final result of the PSO segmented image. The accuracy test for Fig. 5 is 97.63% and for Fig. 6, it is 97.41%. The accuracy for *k*-means segmentation for Fig. 5 is 97.63% and 97.41%. For the image segmented by the hybrid method, the result of similarity percentage for Fig. 5 is 95.80% and 93.53% for Fig. 6.

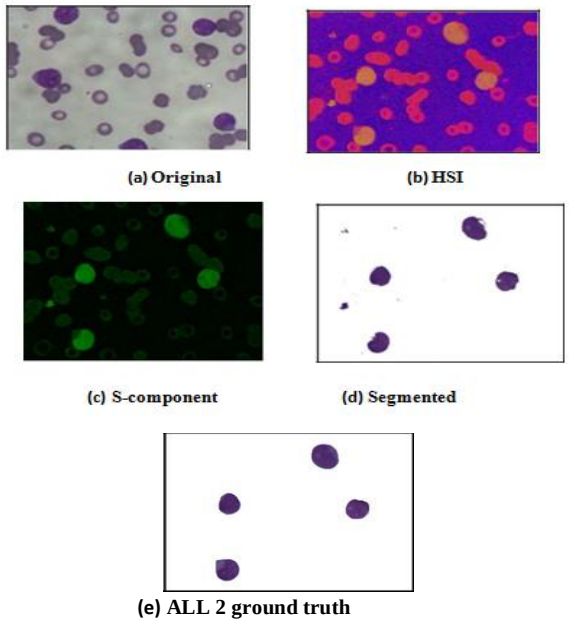

Fig. 5 AML 1 images: (a) Original (b) HIS (c) S-component (d) Segmented (e) AML 2 ground truth

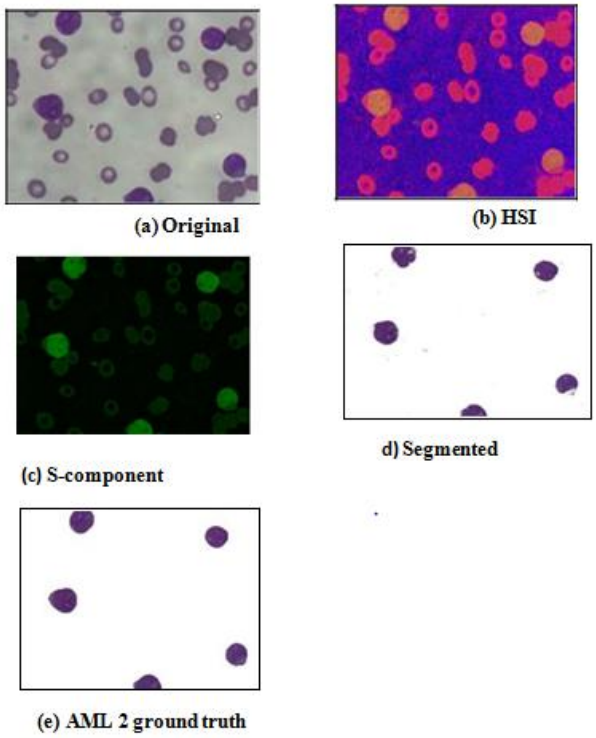

Fig. 6 AML 2 images: (a) Original (b) HIS (c) S-component (d) Segmented (e) AML 2 ground truth

For this hybrid method, after the S-component extraction from the HSI colour model image, the image was first segmented by the *k*-means method and then by the PSO. The product of segmentation by this hybrid *k*-means-PSO method for ALL are as shown in Figure 7(d) and 8(d). To check the accuracy of the segmented image, the ground truth images in Figure 7(e) and 8(e) were used as a reference to calculate the percentage of similarity. The accuracy of the segmented image was evaluated by the SSIM program. The percentage of similarity between the segmented image for Figure 7 is 98.53% and 98.29% for Figure 8.

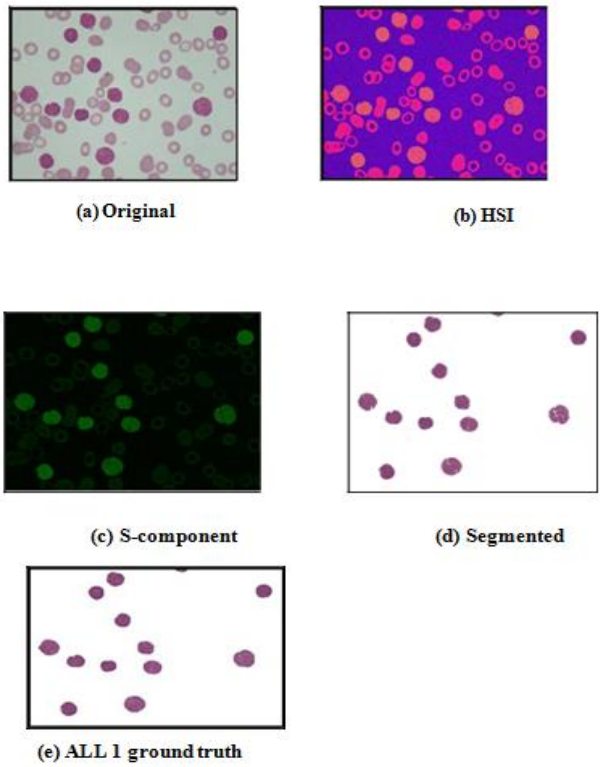

Fig. 7 ALL 1 images: (a) Original (b) HIS (c) S-component (d) Segmented (e) ALL 1 ground truth

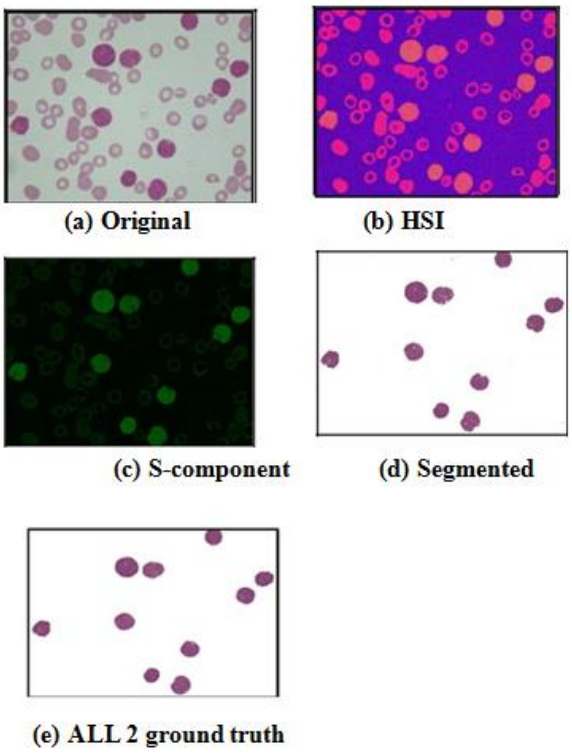

Fig. 8 ALL 2 images: (a) Original (b) HIS (c) S-component (d) Segmented (e) ALL 2 ground truth

As for AML, the original image is as shown in Figure 9(a) and 10(a). The HSI that was converted for this sample are as displayed in Figure 9(b) and 10(b). S-component was extracted and the images are as shown in Figure 9(c) and 10(c). Then, Figure 9(d) and 10(d) show the final result of the hybrid *k*-means-PSO segmented images. The accuracy test for Figure 9 is 95.80% and 93.53% for Figure 10.

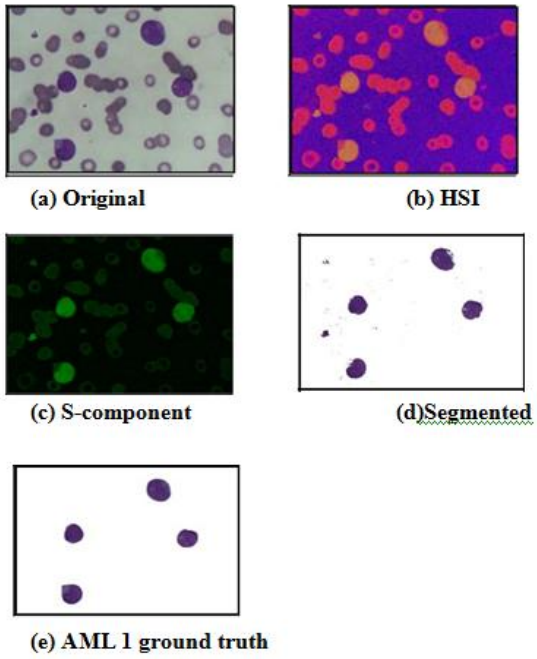

Fig. 9 AML 1 images: (a) Original (b) HIS (c) s-Component (D) Segmented (e) AML 1 ground truth

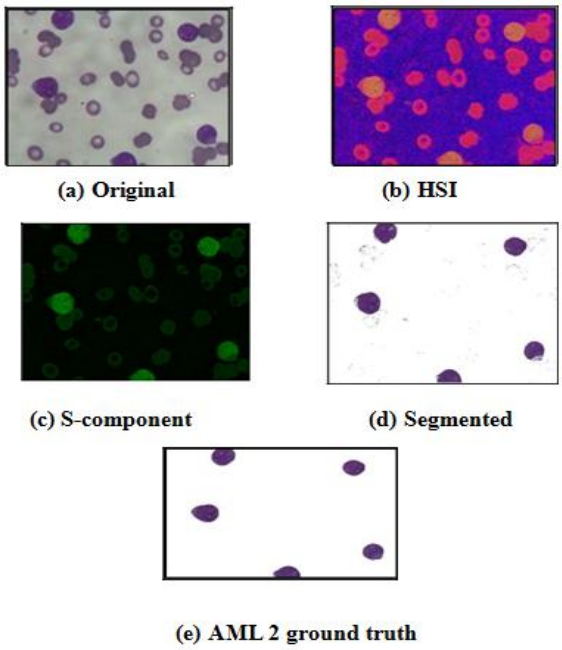

Fig. 10 AML 2 images: (a) Original (b) HIS (c) S-component (d) Segmented (e) AML 2 ground truth

Based on the results obtained, it can be seen that there are differences in performance between the conventional *k*-means method, PSO only method and the hybrid *k*-means-PSO method. Figure 11 and 12 show the visual differences of the segmented image between the three methods. Figure 11 shows the ALL blood image with the segmented result, while Figure 12 shows the image of AML with the segmented image obtained based on the three methods. As shown in both Figure 11 and 12, the segmented images produced by the three methods are quite identical. However, there is a small difference for each image obtained. Figure 11 shows the image of ALL. From the original image of ALL shown in Figure 11(a), the segmented image produced by the conventional *k*-means method are shown in Figure 11(b). Figure 11(c) illustrates the image produced using the PSO only method while the segmented image produced by the hybrid *k*-means-PSO are as shown in Figure 11(d). Visually, the image produced does not have much difference if seen with the naked eye. Using the SSIM, the evaluation for the image has been made and the ground truth image is used as a reference. For the image of ALL in Figure 11, the similarity index for *k*-means segmented image is 97.59%. For the segmented image produced by the PSO only and hybrid method, the similarity index is 97.93% and 98.50% respectively. The hybrid method shows the best performance compared to the other two methods.

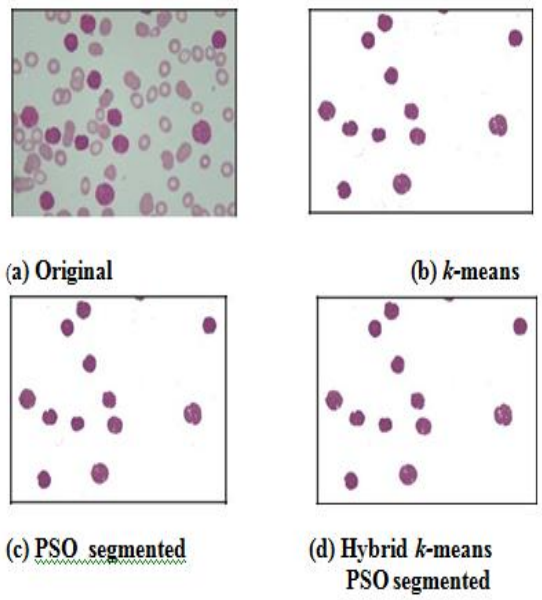

Fig. 11 ALL images: (a) Original (b) k-means segmented (c) PSO segmented (d) Hybrid k-means-PSO segmented

Evaluation for the image has been made and the ground truth image is used as a reference. For the image of ALL in Figure 11, the similarity index for *k*-means segmented image is 97.59%. For the segmented image produced by the PSO only and hybrid method, the similarity index is 97.93% and 98.50% respectively. The hybrid method shows the best performance compared to the other two methods.

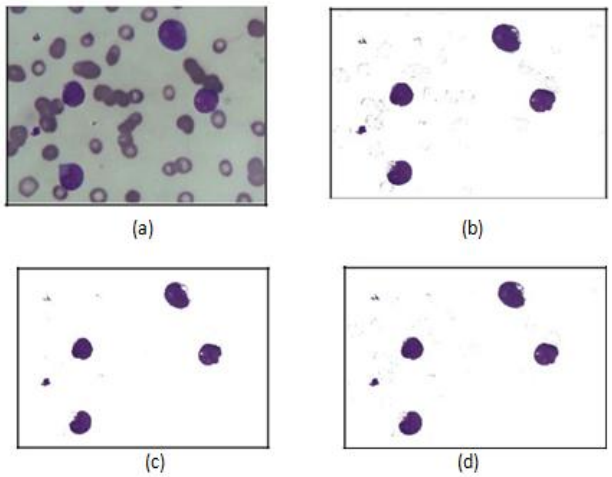

Fig. 12 AML images: (a) Original (b) k-means segmented (c) PSO segmented (d) Hybrid k-means-PSO segmented

On the other hand, Figure 12 shows the image of AML. From the original image of AML shown in Figure 12(a), the segmented image produced by the conventional *k*-means method are shown in Figure 12(b). Figure 12(c) illustrates the image produced by using the PSO only method, and the segmented image produced by the hybrid *k*-means-PSO is shown in Figure 12(d). Even though the image produced does not have much difference visually, the evaluation made by SSIM shows a difference in similarity index value when compared to the ground truth image. For the image of AML in Figure 12, the similarity index for *k*-means segmented image is 92.80%. For the segmented image produced by the PSO only and hybrid method, the similarity index is 97.63% and 95.80% respectively. Unlike ALL in Figure 11, for AML the segmented image produced by the PSO only method shows the best performance compared to the other two methods.

Tables 1 and 2 show the accuracy result for all the tested images.

Table. 1 ALL accuracy test

Image	*K*-means Accuracy (%)	PSO Accuracy (%)	Hybrid Accuracy (%)
1	96.95	**98.76**	98.59
2	96.91	97.88	**98.29**
3	95.64	**98.27**	98.24
4	96.79	97.79	**97.99**
5	97.59	97.93	**98.50**
6	97.78	**98.19**	98.16
7	99.08	98.86	**99.36**
8	97.52	97.53	**97.59**
9	95.21	96.22	**96.33**
10	93.71	93.98	**94.0**
Average	96.72	97.54	**97.71**

As per Table 1, it is evident that the segmented ALL image produced by the hybrid *k*-means-PSO technique was of higher quality than either method alone. The enhancement of the conventional *k*-means method using PSO seems to be more accurate and reliable in producing segmented images. This can be very useful in acute leukemia detection.

However, the outcomes for the hybrid method seemed to be different for ALL and AML. On the other hand, as shown in Table 2, the result for the AML image segmentation is more reliable for the PSO than for the hybrid method. The difference of the results obtained for ALL and AML might be due to the tone of colour of the original image captured and the types of acute leukaemia itself.

Table. 2 AML accuracy test

Image	*k*-means accuracy (%)	PSO accuracy (%)	Hybrid accuracy (%)
1	92.50	**95.58**	94.94
2	94.90	**97.93**	97.01
3	95.95	97.07	**97.15**
4	93.91	**97.76**	96.86
5	96.47	**97.84**	97.47
6	93.70	**96.28**	95.53
7	92.60	**95.94**	95.57
8	89.89	**95.45**	93.39
9	93.85	**97.03**	96.13
10	94.48	**96.35**	96.20
11	94.04	95.24	**95.33**
12	96.16	**96.64**	96.60
13	91.22	**96.65**	94.92
14	93.25	**95.96**	95.37
15	91.55	**96.00**	94.29
16	96.62	**98.12**	97.85
17	92.80	**97.63**	95.80
18	96.78	97.51	**97.89**
19	94.44	95.81	**95.89**
20	89.27	**97.41**	93.53
21	98.54	98.44	**98.69**
22	98.30	97.91	**98.42**
23	98.24	98.32	**98.67**
24	97.41	97.58	**98.19**
Average	94.45	**96.94**	96.32

Table 3 shows the average results for both AML and ALL in terms of the accuracies of the *k*-means, PSO, as well as the combinatory methods. The overall result shows that the best performance in image segmentation for acute leukemia is by using the PSO. The proposed method of using PSO produced a better result than the conventional method of *k*-means. In terms of accuracy, PSO is more reliable and stable in producing a great segmented image of the blood sample. However, besides the pros there are also the cons of PSO that can be improved in the future. The time taken for PSO to complete the image segmentation took quite some time. For the test that was done, the time taken for the process was around 20s for each session of the PSO image segmentation. There were a few things that led to the delay. Firstly, the size of the image is 800x600 pixels which is equal to 480,000 pixels to be processed. Secondly, the number of particles assigned for the process also influences the time taken. Besides that, the number of iterations is one of the reasons that make the processing of the image time-consuming.

Table. 3 Average performance of ALL and AML

Image	*k*-means accuracy (%)	PSO accuracy (%)	Hybrid accuracy (%)
ALL	96.72	97.54	**97.71**
AML	94.45	**96.94**	96.32
Average	95.59	**97.24**	97.02

For *k*-means segmentation, it took only about 2s to obtain the result which is about ten times faster compared to PSO. As for the hybrid, in light of the fact that it was an amalgamation of the two techniques, the duration of the process is quite similar to the PSO. The reasons are similar to the PSO method. Besides that, it was expected for the hybrid method to be of higher accuracy vis-à-vis either of its constituent techniques owing to the abovementioned reason. For this method, the *k*-means will calculate the value of the centroid for the image segmentation and PSO is supposed to use that value and optimize it instead of self-finding using a random value for the centroid. The optimized value was supposed to produce a better result since both methods were combined. In this case, for the overall results, the accuracy for hybrid is better than *k*-means. Unexpectedly, as compared to PSO the accuracy is better for the ALL image segmentation, and vice versa for the AML image segmentation.

IV. CONCLUSION

The empirical evidence of the study indicates that the segmentation of Leukemia image using PSO obtain the highest accuracy.. With reference to the HSI color model, the *S*-component was selected since the characteristics seemed to be better and were able to provide more information compared to the other two components of hue and intensity.

For ALL, the best performance was archived (97.71%) when the hybrid k-means-PSO method was utilized. In fact, 70% of the results by this hybrid method is better than those from the individual method or PSO.

For AML, the results established that the best performance was shown by the PSO method. The image used for this type of acute leukemia is 24. 67% of the test

showed the best result when using the PSO method. The average performance of PSO for AML is 96.94%.

The overall performance for the acute leukemia image segmentation shows the best for the PSO method with the average accuracy of 97.24%. It is proven that the PSO method image segmentation produced better performance of accuracy compared to the conventional *k*-means method and thus, it is regarded as reliable in acute leukemia detection.

For improvement, the time taken for the process can be reduced as the aim of this proposed technique was to come up with a quick and straightforward technique to segment blood images. Additionally, for future work, this proposed method is a platform that enables the conduct of further studies on acute leukemia detection. For the segmented image, the count of defect WBC should be proposed as it is one of the important criteria in the diagnosis of the leukemia disease.

V. ACKNOWLEDGEMENT

This research was sponsored by the Research Acculturation Grant Scheme (RAGS) (s/o code: 13266). The authors would like to thank the members of the leukemia research team at University Malaysia Perlis (UniMAP) for making this research achievable, Hospital University Sains Malaysia (HUSM) for supplying the acute leukemia blood samples and University Utara Malaysia for supporting this research.

REFERENCES

1. N. H. Harun, Y. Mashor, N. R. Mokhtar, and M. K. Osman, "Comparison of Acute Leukemia Image Segmentation using," *International Conference on Information Science, Signal Processing and their Applications*, vol. 10, pp. 749-752, 2010.
2. G. C. C. Lim, "Overview of Cancer in Malaysia," *Japanese Journalof Clinical Oncology*, vol. 32, pp. S37-S42, 2002.
3. H. Lim, E. Francis, M. Mashor, and R. Hassan, "Application of watershed segmentation on RGB and HSI model," in *InternationalConference of Robotic Automation System (ICORAS)*, 2011, pp.134-138.
4. N. H. A. Halim, M. Y. Mashor, A. S. Abdul Nasir, N. R. Mokhtar, and H. Rosline, "Nucleus segmentation technique for acute leukemia," *Proceedings - 2011 IEEE 7th International Colloquiumon Signal Processing and Its Applications, CSPA 2011*, pp. 192-197, 2011.
5. A.S. Abdul Nasir, M. Y. Mashor, and H. Rosline, "Unsupervised colour segmentation of white blood cell for acute leukaemia images," *2011 IEEE International Conference on Imaging Systemsand Techniques, IST 2011 - Proceedings*, pp. 142-145, 2011.
6. S. Miwa, *Atlas of blood cell*. Tokyo: Bunkodo, 1998.
7. Panovska-Stavridis, L. Cevreska, S. Trajkova, L. Hadzi-Pecova, D. Trajkov, A. Petlichkovski, *et al.*, "Preliminary results of introducing the method multiparameter flow cytometry in patients with acute leukemia in the Republic of Macedonia," *MacedonianJournal of Medical Sciences*, vol. 1, pp. 36-43, 2008.
8. S. Mohapatra, D. Patra, S. Kumar, and S. Satpathi, "Kernel Induced Rough c-means clustering for lymphocyte image segmentation," *4thInternational Conference on Intelligent Human Computer Interaction: Advancing Technology for Humanity, IHCI 2012*, 2012.
9. R. Bhattacharjee and L. M. Saini, "Detection of Acute Lymphoblastic Leukemia using watershed transformation technique," in *Signal Processing, Computing and Control (ISPCC),2015 International Conference on*, 2015, pp. 383-386.
10. S. Mohapatra, S. S. Samanta, D. Patra, and S. Satpathi, "Fuzzy based blood image segmentation for automated leukemia detection," in *Devices and Communications (ICDeCom), 2011International Conference on*, 2011, pp. 1-5.
11. M. M. D. Joshi, A. H. Karode, and S. Suralkar, "White blood cells segmentation and classification to detect acute leukemia," *International Journal of Emerging Trends and Technology in Computer Science (IJETICS)*, vol. 2, 2013.
12. E. A. Mohammed, B. H. Far, M. M. Mohamed, and C. Naugler, "Application of support vector machine and *k*-means clustering algorithms for robust chronic lymphocytic leukemia color cell segmentation," in *e-Health Networking, Applications & Services(Healthcom), 2013 IEEE 15th International Conference on*, 2013,pp. 622-626.
13. N. H. Harun, M. Y. Mashor, and A. Azamimi, "Segmentation Technique of Blast in Acute Leukaemia Blood Slide Images Based on K Means Clustering Procedure."
14. C. W. Chen, J. Luo, and K. J. Parker, "Image segmentation via adaptive *K*-mean clustering and knowledge-based morphological operations with biomedical applications," *IEEE Transactions onImage Processing*, vol. 7, pp. 1673-1683, 1998.
15. F. Mohsen, M. Hadhoud, K. Mostafa, and K. Amin, "A New Image Segmentation Method Based on Particle Swarm Optimization," *TheInternational Arab Journal of Information Technology*, vol. 9, pp.487-493, 2012.
16. S. Ait-a, "Medical Image Seg gmentation using Particle Swarm Op ptimization," 2014.
17. D. Van der Merwe and A. P. Engelbrecht, "Data clustering using particle swarm optimization," in *Evolutionary Computation, 2003.CEC'03. The 2003 Congress on*, 2003, pp. 215-220.
18. A. Mekhmoukh and K. Mokrani, "Improved Fuzzy C-Means based Particle Swarm Optimization (PSO) initialization and outlier rejection with level set methods for MR brain image segmentation," *Computer Methods and Programs in Biomedicine*, vol. 122, pp.266-281, 2015.
19. P. Ghamisi, M. S. Couceiro, F. M. Martins, and J. A. Benediktsson, "Multilevel image segmentation based on fractional-order Darwinian particle swarm optimization," *IEEE Transactions onGeoscience and Remote sensing*, vol. 52, pp. 2382-2394, 2014.
20. M. H. Moradi and M. Abedini, "Electrical Power and Energy Systems A combination of genetic algorithm and particle swarm optimization for optimal DG location and sizing in distribution systems," *International Journal of Electrical Power and EnergySystems*, vol. 34, pp. 66-74, 2012.
21. WorawutSrisukkham, Li Zhang, Siew Chin Neoh, StephenTodryk, Chee Peng Lim, "Intelligent leukaemia diagnosis with bare-bones PSO based feature optimization," *Applied Soft Computing*, vol. 56, pp. 405-419, 2017.
22. P. Agarwalla& S. Mukhopa, "Multiswarm Selection of Relevant Genes for Pediatric Leukemia using Co-Operative," *MaterialsToday: Proceedings*, vol. 3, Issue 10, Part A, pp. 3328-3336, 2016.
23. H. Nor Hazlyna, "Sistemsaringan dan diagnosis automatikpenyakit leukemia akutberasaskansampeldarah," Ph.D., Electronic & Biomedical Intelligent Systems (EBItS) Research Group, School of Mechatronic Engineering, Universiti Malaysia Perlis, 2013.
24. M. Omran, A. Salman, and A. P. Engelbrecht, "Image classification using particle swarm optimization," in *Proceedings of the 4th Asia-Pacific conference on simulated evolution and learning*, 2002, pp.18-22.